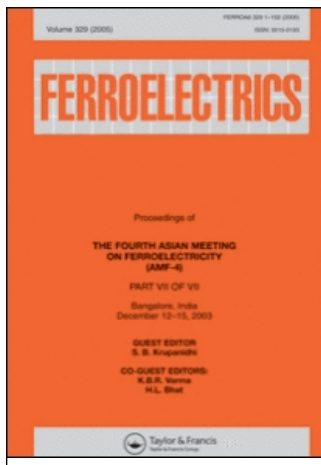


This article was downloaded by:[Canadian Research Knowledge Network]  
On: 21 July 2008  
Access Details: [subscription number 783016891]  
Publisher: Taylor & Francis  
Informa Ltd Registered in England and Wales Registered Number: 1072954  
Registered office: Mortimer House, 37-41 Mortimer Street, London W1T 3JH, UK



## Ferroelectrics

Publication details, including instructions for authors and subscription information:  
<http://www.informaworld.com/smpp/title~content=t713617887>

### A novel PVDF thin-film photopyroelectric thermal-wave interferometry

Andreas Mandelis<sup>a</sup>; Chinhua Wang<sup>a</sup>

<sup>a</sup> Department of Mechanical and Industrial Engineering, University of Toronto, Photothermal and Optoelectronic Diagnostics Laboratories (PODL), Toronto, Ontario, Canada

Online Publication Date: 01 January 2000

To cite this Article: Mandelis, Andreas and Wang, Chinhua (2000) 'A novel PVDF thin-film photopyroelectric thermal-wave interferometry', *Ferroelectrics*, 236:1, 235 — 246

To link to this article: DOI: 10.1080/00150190008016055

URL: <http://dx.doi.org/10.1080/00150190008016055>

PLEASE SCROLL DOWN FOR ARTICLE

Full terms and conditions of use: <http://www.informaworld.com/terms-and-conditions-of-access.pdf>

This article maybe used for research, teaching and private study purposes. Any substantial or systematic reproduction, re-distribution, re-selling, loan or sub-licensing, systematic supply or distribution in any form to anyone is expressly forbidden.

The publisher does not give any warranty express or implied or make any representation that the contents will be complete or accurate or up to date. The accuracy of any instructions, formulae and drug doses should be independently verified with primary sources. The publisher shall not be liable for any loss, actions, claims, proceedings, demand or costs or damages whatsoever or howsoever caused arising directly or indirectly in connection with or arising out of the use of this material.

# A Novel PVDF Thin-Film Photopyroelectric Thermal-Wave Interferometry

ANDREAS MANDELIS and CHINHUA WANG

*Photothermal and Optoelectronic Diagnostics Laboratories (PODL), Department of Mechanical and Industrial Engineering, University of Toronto, Toronto, Ontario M5S 3G8, Canada*

*(Received July 12, 1999)*

A purely thermal-wave interferometric technique based on two-cavity photopyroelectric (PPE) detection using a thin film polyvinylidene fluoride (PVDF) has been developed. The interfering thermal waves within the PVDF thin film are generated by two intensity-modulated laser beams which pass through a sample and a reference medium and are incident onto the two active surfaces of the PVDF thin film from the opposite directions. The capabilities of this interferometry are investigated with a general theory. Applications of this technique to differential measurements of optical properties of solid laser crystals, thermal diffusivity of air and the detection of trace hydrogen in nitrogen were carried out and were compared with the conventional methods. The major feature of the technique is the efficient suppression of the background PPE signal and, therefore, significant enhancement of the measurement sensitivity, precision, and signal dynamic range.

*Keywords:* pyroelectric thin film; thermal-wave interferometry; thermal diffusivity; hydrogen sensor

## 1. INTRODUCTION

As one branch of the photothermal and photoacoustic family, the single-beam photopyroelectric (PPE) technique is a well-established photothermal method used for spectroscopic and thermal characterization of various materials as well as for studies of thermophysical properties of gases<sup>1-9</sup>. The basic principle of the single-beam PPE technique is that when a periodically modulated energy source impinges on the surface of a sample, the sample will absorb

some of the incident energy and will, in turn, produce a localized temperature increase following a non-radiative de-excitation process. This periodic temperature variation in the sample can be detected with a pyroelectric transducer made of a thin-film pyroelectric material (e.g. polyvinylidene fluoride, PVDF). If the sample does not contact the transducer, the air gap formed in the medial region amounts to a thermal-wave cavity. This cavity confines the thermal-wave oscillation and has been shown to give rise to a standing-wave-equivalent structure, the length of which can be tuned to resonant antinode and node patterns<sup>5</sup>. Recently, such thermal-wave resonant cavities have been used for high precision measurements of thermophysical properties of the intracavity gases<sup>5,8,9,11</sup>.

In all the conventional embodiments of the PPE technique<sup>1,4,7,10</sup>, a single excitation source is employed with the radiation impinging on either the front- (PPE), or the rear-surface (Inverse PPE, IPPE) of a PVDF transducer. The sensitivity and dynamic range, however, of the PPE measurement scheme can be compromised in the study of solid transparent materials, due to the substantial baseline signal from direct transmission of the incident light onto the detector. Moreover, the fluctuation of incident light also introduces a large optical noise to the measurement in the single-beam measurement scheme.

In this work, we have developed a new purely-thermal-wave interferometric technique. The unique characteristic of the purely-thermal-wave interferometry is that the technique is based on the spatial interference of thermal-waves *within the body of the pyroelectric transducer*, independently of the sample. Unlike other prior ("conventional") photothermal interferometric schemes<sup>12-15</sup>, the new technique is *not* based on monitoring thermal waves resulting from direct optical interference patterns, such as those generated by two appropriately modulated laser beams (e.g. intensity, phase or polarization modulation). In the present coherence scheme, thermal waves interfere as they are induced by two intensity-modulated beams, split-off a single laser source and with a fixed phase-shift relationship between them. The usually large instrumental PPE baseline signal and a significant portion of the noise can be efficiently suppressed within the PVDF detector if the two laser beams are collinearly incident on opposite surfaces of the thin pyroelectric film, and with 180° relative phase shift. In this fashion, much higher signal sensitivity and dynamic range PPE measurements than with the conventional single-beam PPE configurations are expected and have been confirmed very recently in this Laboratory<sup>16</sup>. This paper presents a generalized theory of a purely thermal-wave interferometry and several applications which have been

implemented for different research aspects including measurement of optical properties of solid laser crystals, measurement of thermal diffusivity of air, and the design and development of a novel H<sub>2</sub> gas sensor.

2. A GENERALIZED THEORY OF PPE PURELY-THERMAL-WAVE INTERFEROMETRY

The most general configuration diagram for purely-thermal-wave PPE interferometry using a one-dimensional heat transfer model is shown in Fig.1. Two laser beams of intensities  $I_1$  and  $I_2$ , respectively, are split off of a laser source and are modulated at the same angular frequency ( $\omega$ ). They have a fixed, adjustable phase shift ( $\Delta\phi$ ), and are incident

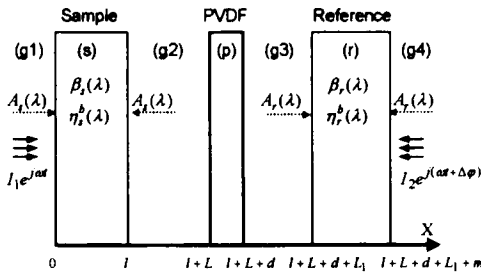


FIGURE 1 Schematic of a photopyroelectric interferometry for theoretical analysis.

onto the front- and rear-surfaces of a PVDF detector, passing through optically transparent sample and reference media, which, along with the PVDF sensor in the middle form the thermal-wave cavities g2 and g3 as shown in Fig.1. The sample and the reference have bulk optical absorption coefficient  $\beta_s, \beta_r$ , surface absorptance  $A_s, A_r$ , and surface and bulk non-radiative energy conversion efficiency,  $\eta_s^b(\lambda), \eta_r^b(\lambda)$ , respectively. Light absorption by the sample-PVDF-reference system and nonradiative energy conversion to heat increases the temperature of the PVDF sensor, which results in a potential difference between the two surfaces of the transducer due to the photopyroelectric effect. The photopyroelectric signal from the PVDF detector is proportional to the average ac temperature of the PVDF film detector<sup>7</sup>, and can be written:

$$V(\omega) = S(\omega) \int_{l+L}^{l+L+d} T_p(x, \omega) dx \quad (1)$$

Here  $S(\omega)$  is the instrumental transfer-function, which is usually normalized out by means of experimental procedures.  $T_p(x, \omega)$  is the local complex thermal-wave field in the PVDF, which must be calculated from coupled one-dimensional heat diffusion equations subject to appropriate boundary conditions across each interface (g1-S, S-g2, g2-P, P-g3, g3-R, and R-g4) of Fig. 1. In the most general theoretical treatment, gaseous media of different thermophysical properties are assumed to exist in regions g1, g2, g3, and g4. Following the same procedure as that in Ref.(17), the output photopyroelectric signal (voltage mode) for the geometry of Fig.1 can be finally expressed as follows:

$$V(\omega) = \frac{S(\omega)}{\sigma_p(1+b_{2p})(1+b_{3p})} \times \frac{H_1(1+b_{3p})\{G_1(1+W_{21}e^{-2\sigma_2 L})+2b_{2p}G_3e^{-\sigma_2 L}\}+H_2(1+b_{2p})\{G_2(1+V_{34}e^{-2\sigma_3 L})+2b_{3p}G_4e^{-\sigma_3 L}\}}{[e^{\sigma_p d}(1+\gamma_{3p}V_{34}e^{-2\sigma_3 L})(1+\gamma_{2p}W_{21}e^{-2\sigma_2 L})-e^{-\sigma_p d}(\gamma_{2p}+W_{21}e^{-2\sigma_2 L})(\gamma_{3p}+V_{34}e^{-2\sigma_3 L})]} \quad (2)$$

where  $\sigma_i = (1+j)\sqrt{\omega/2\alpha_i}$  is the complex thermal diffusion coefficient in region  $i$  ( $i = \text{g1, g2, g3, g4, S, P, R}$ ) with thermal diffusivity  $\alpha_i$ ; and  $b_{ij} = k_i\sqrt{\alpha_j}/k_j\sqrt{\alpha_i}$ ,  $\gamma_{ij} = (1-b_{ij})/(1+b_{ij})$ ,

$$W_{21} = -\frac{\gamma_{2s}e^{\sigma_s l} - \gamma_{1s}e^{-\sigma_s l}}{e^{\sigma_s l} - \gamma_{2s}\gamma_{1s}e^{-\sigma_s l}}, \quad V_{34} = -\frac{\gamma_{3r}e^{\sigma_r m} - \gamma_{4r}e^{-\sigma_r m}}{e^{\sigma_r m} - \gamma_{3r}\gamma_{4r}e^{-\sigma_r m}},$$

$$G_1 = \frac{(1-R_p)}{k_p\sigma_p} \times \frac{I_1(1-R_s)^2}{1-R_s^2 e^{-2(\beta_s l + A_s)}} e^{-(\beta_s l + 2A_s)},$$

$$G_2 = \frac{(1-R_p)}{k_p\sigma_p} \times \frac{I_2 e^{j\Delta\phi}(1-R_r)^2}{1-R_r^2 e^{-2(\beta_r m + A_r)}} e^{-(\beta_r m + 2A_r)}.$$

$k_i$  and  $R_i$  are the thermal conductivity and the surface optical reflectivity of medium  $i$ , respectively. Expressions for  $H_1, H_2$  and  $G_3, G_4$  are given in Ref (17). From the structure of the PPE output voltage of Eq. (2), it can be seen that the first term in the numerator represents the contribution from the front beam, through the sample and the intracavity gas layer g2. The second term originates from the rear incident beam, through the reference layer and the intracavity gas layer

g3. Therefore, the overall output signal is the result of the complex (vectorial) superposition of two thermal wave fields within the PVDF detector generated by two incident laser beams of equal fluences modulated with a fixed phase shift  $\Delta\varphi$ . Eq.(2) gives the most general expression for thermal-wave interferometry. In practice, however, this expression can be further simplified by using appropriate combinations of the samples and incident beams.

### 3. APPLICATIONS OF THE PPE INTERFEROMETRIC TECHNIQUE

A schematic of the PPE interferometry is shown in Fig. 2. At the heart of this interferometer lie two thermal-wave cavities formed by sample-pyroelectric and pyroelectric-reference compartments. The PVDF thin film detector, 52- $\mu\text{m}$ -thick and 2-cm in diameter, was installed on an aluminum-base bearing a hole. The PVDF element acts as a thermal-wave signal transducer and as a wall for front and back thermal-wave cavities. Both sample and reference are mounted on a 3-D angularly and linearly adjustable micrometer stage of 10- $\mu\text{m}$  resolution in linear motion and 0.1 degree in angular rotation. The relative intensities of the front and back incident beams, which are split off of a He-Ne laser ( $\lambda = 632.8 \text{ nm}$ ,  $P \approx 10\text{mW}$ ), are adjusted by a linear intensity attenuator, and the phase shift between the two beams is precisely controlled by a mechanical chopper (EG&G Model 192), also fixed on a micrometer stage. The experimental data are collected by a PC via a lock-in amplifier (EG&G Model 5210). By using different configurations of the samples and appropriate coatings on the PVDF surfaces, we can differentially measure the optical properties of the solid sample, the thermal properties of the constituents in the cavity and construct a highly sensitive  $\text{H}_2$  sensor.

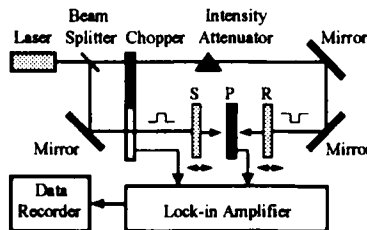


FIGURE 2 Experimental setup for PPE thermal-wave interferometry. S: sample, P: PVDF detector, R: reference

### 3.1 Deconvolution Measurement of Bulk and Surface Optical Absorptions in Ti:sapphire Crystals Using PPE Interferometry

In view of Eq.(2), the overall output PPE signal is affected by the surface absorptances as well as by the bulk absorption coefficients of the sample and the reference. By using appropriate combinations of pairs of samples, in which only one parameter (surface absorptance, bulk absorption or thickness) varies between a sample-reference pair, one may precisely measure the variation of this parameter without requiring accurate information about the values of other parameters.

Several pairs of Ti-sapphire crystals were used in the role of sample and reference in our experiments. Fig. 3 shows the experimental results of two samples with identical bulk but different surface quality. The crystal with "good" surface polish (thickness  $l = 0.0771\text{cm}$ ) was used as the sample, and the crystal with "non-optimal" polish (thickness  $m = 0.0810\text{cm}$ ) was used as the reference. The modulation frequency was  $f = 26.5\text{Hz}$ . In the experiment, the reference was placed in the deep PPE mode<sup>17</sup> (very close to the PVDF detector). By fitting the experimental data of the amplitude channel to the theoretical formula, Eq.(2), the difference in surface absorptance between the sample and the reference ( $\Delta A = A_s - A_r$ ) was found to be  $0.0113 \pm 0.0002$ . The cavity length,  $L_l$ , between the PVDF film and the reference was  $0.213 \pm 0.002\text{ mm}$ , the average of three measurements. The PPE signal phase was then calculated using  $\Delta A$  and  $L_l$  obtained from the amplitude fit to ascertain consistency and validity.

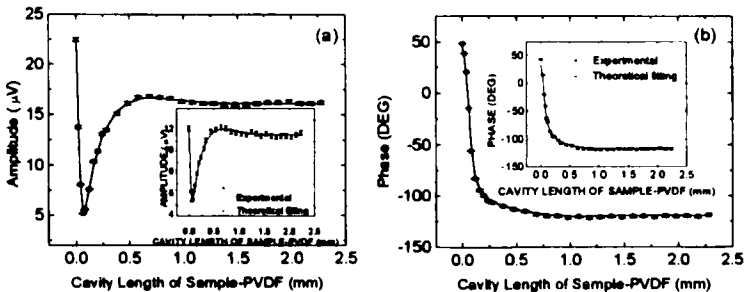


FIGURE 3 Experimental and theoretical (fitted) results of (a) the amplitude and (b) phase for a pair of Ti:sapphire crystals with identical bulk optical properties, but different surface polish. Solid squares: experimental; solid lines: theoretical fits. Insets: experimental and theoretical fit results for the same pair of samples, when the reference was placed farther away from the PVDF sensor.

To check the sensitivity and to validate the measurement, the reference was subsequently moved farther away from the detector by 0.05 mm and the experiment was repeated. The measurement curves are shown in the insets of Figs. 3(a) and (b) for the amplitude and the phase, respectively. The fitted values for  $\Delta A$  and  $L_I$  at this position were  $0.0116 \pm 0.0005$ , and  $0.267 \pm 0.003$  mm, respectively. It can be seen that both measurements gave very consistent values, the relative error between the two measurements being only 2.7% for  $\Delta A$ . The fitted value *difference* for the cavity length  $L_I$  between the two measurements is 0.054 mm, in excellent agreement with the actual scanned distance of 0.05 mm.

In the foregoing fitting process, it was found that the dependence of the fitted value  $\Delta A$  on the initial value of the bulk absorption coefficient ( $\beta_s = \beta_r$ ) and the surface reflectivity ( $R_s = R_r$ ) is trivial. This is an important feature of the interferometric PPE technique which is different from the conventional one<sup>18</sup>. It implies that for the purpose of measuring the difference of surface absorptances between two crystals of the same (or nearly equal) thickness and bulk optical quality, it is not necessary to know the exact value of the bulk absorption coefficient.

Fig.4 shows the experimental results of two samples with different bulk optical properties (FOM), but identical surface preparation. One Ti:Sapphire crystal (FOM = 800) of thickness  $l = 2.013$  cm was used as the sample. The other crystal (FOM = 40) of thickness  $m = 2.017$  cm was used as the reference. The modulation frequency was 10 Hz. In the experiment, the reference was placed in the thermally uncoupled (OT)<sup>19</sup> mode. By fitting the experimental results to the theoretical Eq.(2), the difference of the bulk absorption coefficient between the FOM = 40 and the FOM = 800 Ti:Sapphire crystals was found to be:  $\Delta\beta = \beta_r - \beta_s = 0.0545 \pm 0.0006 \text{ cm}^{-1}$ , the average of four measurements.

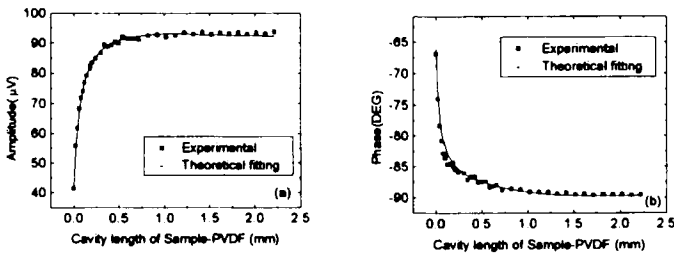


FIGURE 4 Experimental and theoretical (fitted) results of (a) the amplitude and (b) phase for a pair of Ti:sapphire crystals with identical surface polishes, but different bulk optical properties.



The cavity length  $L_1$  was found to be greater than 8 mm for all three measurements. This best-fit result is consistent with the experimental arrangement, in which the reference was actually placed in the OT mode. Both amplitude and phase fits to the data are excellent, as shown in Figs. 4 (a) and (b). Once again, it is shown that the measurement of bulk  $\Delta\beta$  does not depend strongly on the absolute values of surface absorptance and reflectivity over wide ranges of  $A_s$  and  $R_s$ .

### 3.2 Measurement of Thermal Diffusivity of Air Using PPE Interferometry

In this section, we introduce an application of the PPE interferometric technique in the measurement of thermal diffusivity of a gas. For measuring thermal diffusivity of a gas, a simple experimental configuration can be used, in which the reference is absent; only the sample and two incident beams are employed. As a result, PPE output is only a function of the cavity length  $L$  formed by sample-PVDF. By scanning the cavity length  $L$ , we can fit the experimental data to a simplified theoretical expression of Eq.(2) to obtain the thermal diffusivity of the gas which fills the cavity. The experiment can be performed either in the PPE destructive method (two-beam mode) or in the single-beam method by blocking the rear incident beam. The experimental setup is the same as that shown in Fig.2. In the experiment, a transparent Ti-sapphire disk sample, 0.1295 cm thick was used as a cavity wall and the whole system was exposed to open air. The sample was first placed at a far distance from the PVDF compared with the thermal diffusion length. The relative intensities between the two beams were then adjusted, such that the output PPE signal was zero. Finally the sample-PVDF distance was scanned and the output signal was recorded vs. the cavity length  $L$ .

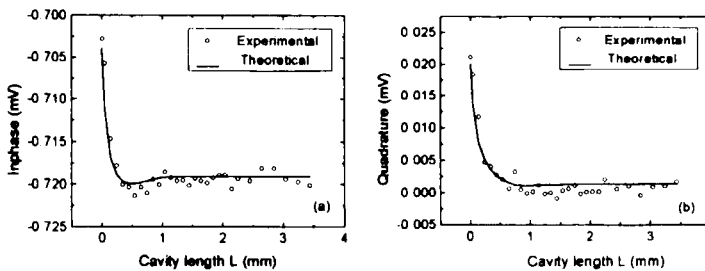


FIGURE 5 PPE experimental data and theoretical fits vs. thermal-wave cavity length  $L$  at a modulation frequency  $f=26.6$  Hz, using single-beam detection with a transparent Ti:sapphire cavity wall.

Fig.5 shows typical experimental results using the single-beam method, in which the rear incident beam was blocked. The modulation frequency,  $f$ , was 26.6 Hz. By fitting the experimental data of the lock-in quadrature channel to the theoretical expression, the thermal diffusivity of room temperature air was found to be  $0.21 \pm 0.02 \text{ cm}^2 \cdot \text{s}^{-1}$ , the average of four measurements. As a comparison, Fig.6 shows experimental results using the destructive interferometric configuration, in which the reference was absent and two laser beams were operating in the PPE destructive mode. It can be seen that the data quality and the SNR are clearly superior to the single-ended case. Fitting the experimental data to theory yielded  $0.219 \pm 0.003 \text{ cm}^2 \text{ s}^{-1}$  as the thermal diffusivity of room-temperature air.

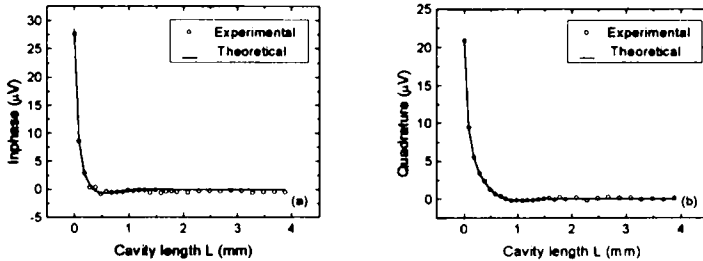


FIGURE 6 PPE experimental and theoretical fits vs thermal-wave cavity length  $L$  at a modulation frequency  $f=26.6\text{Hz}$ , using pure thermal-wave destructive interferometry.

### 3.3 Pd/PVDF Thin Film Hydrogen Sensor Based on PPE Interference

It has been shown that the PPE interferometric technique has a potential application in gas detection due to the zero-background signal under the destructive interference (differential) mode. In this section, we introduce a novel hydrogen gas sensor based on thermal-wave interference.

The basic experimental setup is the same as that shown in Fig. 2. For the purpose of gas detection, we put the PVDF thin film into a test cell and equipped the test cell with a gas supply unit which mixes hydrogen and the background gas in a controlled and homogeneous flow. In the case of hydrogen detection, a PVDF thin film coated with NiAl metals on one surface and Pd metal on the other surface was used. A detailed schematic representation of the test cell is shown in Fig.7. Two laser beams (intensities  $I_1$  and  $I_2$ ), were obtained from a single He-Ne laser beam (15mW) by using a beam splitter. They were modulated with a

mechanical chopper at the same angular frequency ( $\omega$ ) and with a fixed, adjustable phase shift ( $\Delta\phi$ ). One beam was incident onto the

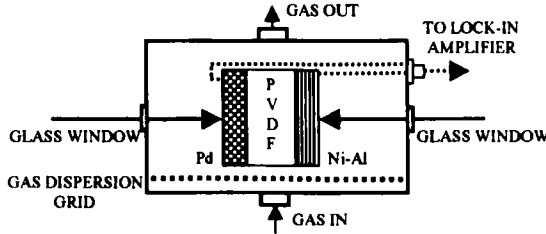


FIGURE 7 Cross-sectional detail of the test cell

front (Pd coating) and the other beam was directed to the rear (NiAl-coated) surface of the PVDF detector from opposite directions. A fully destructive interferometric pattern can be produced when the intensities of the two beams are identical and the phase shift between them is  $180^\circ$ . This destructive operating mode of the PVDF detector yields a sensitive coherent differential method to detect minute changes in the PPE output signal, using a single transducer. It is well known that Pd metal interacts reversibly with hydrogen gas to form a hydride. Associated with these compositional changes are changes in the optical properties, reflectance and absorptance, of the palladium<sup>20,21</sup>. Therefore, a minute change in the PPE output is caused by the change in optical absorptivity of the Pd coating on one surface, while the optical properties of NiAl coating on the other surface remain unchanged before and after exposure to  $H_2$  gas.

Figs.8 (a)-(b) show typical PPE responses as functions of time, using an active element with 53.4-nm-thick Pd, under various hydrogen

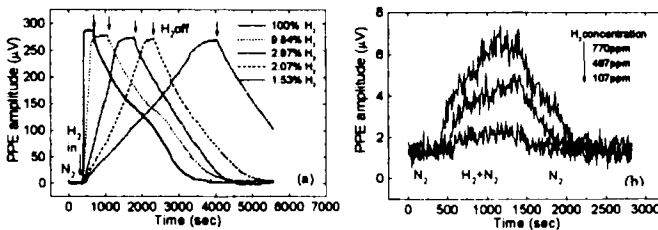


FIGURE 8 PPE signal as a function of time for various concentrations of hydrogen in nitrogen using a Pd-coated (53.4 nm) PVDF film. The gas flow rate was 870 ml/min for all the experiments.

concentrations in  $N_2$  by volume. The modulation frequency was 10 Hz. Fig. 8(b) shows that the detection limit of the 53.4-nm Pd-coated PVDF film is about 100 ppm. As a comparison, the experiments were also conducted using the same sensor, but in the single-beam mode. Fig. 9 shows the experimental results at 0.2% and 0.5% [ $H_2$ ]. The PPE signal change due to the introduction of  $H_2$  is almost entirely embedded in the

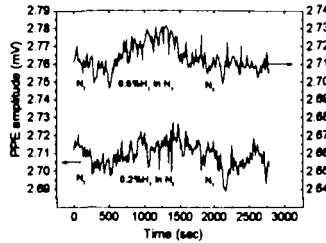


FIGURE 9 PPE signal as a function of time using the single-beam method. The gas flow rate was 870ml/min for both measurements. The two signal traces have been separated out artificially for clarity.

system noise at 0.2%  $H_2$  concentration. The detection limit of the single-beam method is thus believed to be  $>0.2\%$ , yielding approximately 20 times higher interferometric mode detectivity. The foregoing single-beam detection limit is similar to that established earlier with other single-beam optical and photopyroelectric methods<sup>20,22</sup>.

The above experimental results demonstrate the much improved detectivity and much enhanced signal dynamic range, due to the complete suppression of the baseline signal and the system noise, when compared with the single-beam (non-interference) method and other optical methods. Unlike the traditional ratio measurements, in which external electronic devices are used to ratio the signals from two different detectors, this technique exploits the two active surfaces of a single pyroelectric thin film to differentiate the coherent signal within the pyroelectric thin film. This technique provides a completely new methodology for differential measurements in gas sensor applications. It is suitable not only for  $H_2$  gas but for any other gases provided appropriate active coatings are available.

#### 4. CONCLUSION

A novel purely-thermal-wave interferometric technique has been developed. A general theory is presented and several applications have

been discussed. Successful applications of this technique have been implemented in the evaluation of high quality laser crystals, measurement of thermal properties of intracavity gases, and a novel H<sub>2</sub> gas sensor with much higher sensitivity, much lower baseline (theoretically zero baseline), and much larger signal dynamic range than corresponding conventional PPE or optical methods. This methodology/technique has a great potential application in high-resolution optical evaluation/imaging, thin-film studies and gas sensors.

#### ACKNOWLEDGEMENTS

The support of the Natural Sciences and Engineering Research Council of Canada (NSERC) through a Research Grant is gratefully acknowledged.

#### References

- [1] A. Mandelis, *Chem. Phys. Lett.* **108**, 388 (1984); H. Coufal, *Appl. Phys. Lett.* **44**, 59 (1984).
- [2] H. Coufal and A. Mandelis, *Ferroelectrics*, **118**, 379 (1991).
- [3] A. Mandelis, J. Vanniasinkam, and S. Buddhudu, *Phys. Rev. B* **48**, 6808 (1993).
- [4] M. Chirtoc and G. Mihailescu, *Phys. Rev. B* **40**, 9606 (1989).
- [5] J. Shen and A. Mandelis, *Rev. Sci. Instrum.* **66**, 4999 (1995).
- [6] A. Mandelis and K. F. Leung, *J. Opt. Soc. Am. A* **8**, 186 (1991).
- [7] A. Mandelis and M. M. Zver, *J. Appl. Phys.* **57**, 4421 (1985).
- [8] J. Shen, A. Mandelis and B. D. Aloysius, *Int. J. Thermophys.* **17**, 1241 (1996).
- [9] J. Shen, A. Mandelis and H. Tsai, *Rev. Sci. Instrum.* **69**, 197 (1998).
- [10] M. Chirtoc, D. Bicanic and V. Tosa, *Rev. Sci. Instrum.* **62**, 2257 (1991).
- [11] M. Bertolotti, G. L. Liakhou, R. Li Voti, S. Paoloni and C. Sibilina, *Int. J. Thermophys.* **19**, 603 (1998).
- [12] H. Coufal, F. Trager, T. J. Chuang and A. C. Tam, *Surf. Sci.* **145**, L504 (1984).
- [13] Z. Sodnik and H. J. Tiziani, *Opt. Commun.*, **58**, 295 (1986).
- [14] L. Wawrzyniuk and G. Dymny, *Opt. Eng.* **36**, 1602 (1997).
- [15] H. G. Walther, K. Friedrich, K. Haupt, K. Muratikov, and A. Glazov, *Appl. Phys. Lett.*, **57**, 1600 (1990).
- [16] C. Wang and A. Mandelis, *Proc. XI Int. Conf. Photoacoustic & Photothermal Phenomena*, (F. Scudieri, Ed., AIP, New York, 1998).
- [17] C. Wang and A. Mandelis, *J. Appl. Phys.*, **85**, 8366 (1999).
- [18] J. Vanniasinkam, A. Mandelis, S. Buddhudu and M. Kokta, *J. Appl. Phys.* **75**, 8090 (1994).
- [19] C. Wang and A. Mandelis, *Rev. Sci. Instrum.* **70**, 3115 (1999).
- [20] A. Mandelis and J. A. Garcia, *Sensors and Actuators*, **B 49**, 258 (1998).
- [21] F. A. Lewis, *The Palladium/hydrogen System* (Academic, New York, 1967).
- [22] M. A. Butler, *Sensors and Actuators B* **22**, 155 (1994).